



Interferometric measurement of complex-field changes in transient detection imaging

A. ESTEBAN-MARTÍN,^{*}  JAVIER GARCÍA-MONREAL, FERNANDO SILVA, AND GERMÁN J. DE VALCÁRCEL

Departament d'Òptica i Optometria i Ciències de la Visió, Universitat de València, Dr. Moliner 50, 46100-Burjassot, Spain

**adolfo.esteban@uv.es*

Abstract: We report an experimental method that combines nonlinear-crystal-based transient detection imaging (TDI) with interferometric complex-field retrieval. The system allows measuring both phase and amplitude of a dynamic scene while suppressing stationary background. Theoretical and experimental results prove the linear relation existing between input and output phases, as well as the benefits of phase analysis for both detection and measurement with high resolutions of $\lambda/30$, even under noisy conditions. Additionally, we present experimental evidence of the remarkable ability of the technique to detect phase sign changes in the scene—what we call differential-phase TDI—showing great detection sensitivity and no calibration requirements.

© 2020 Optical Society of America under the terms of the [OSA Open Access Publishing Agreement](#)

1. Introduction

A transient detection imaging (TDI) system, also known as optical novelty filter, is a device that detects temporal changes in a scene while suppressing its static parts. Removal of background largely improves the contrast and helps visualizing and measuring intensity and phase information. The most popular TDI systems are based on photorefractive two-wave mixing. Photorefractive materials display a dynamic change of their local refractive index in response to spatial variations of light intensity, typically due to the interference between two coherent beams: the space-charge electric field originated from photoexcitation by the intensity pattern creates, via the linear electro-optic effect, a refractive index grating which is in general spatially shifted from the intensity pattern. As a result, the interfering beams transmit and diffract from the grating and wave coupling is achieved [1–4]. First TDI systems based on photorefractive two-wave mixing were proposed and demonstrated by Cronin-Golomb et al. [5], and theoretically analyzed by Anderson and Feinberg [6]. Photorefractive materials are convenient because they offer large versatility, allowing different wave-mixing configurations, and flexibility in the response time [1]. Optical novelty filters have been used to perform different applications, including object tracking, image subtraction, image differentiation, object comparison and contour generation [7–12]. Notably, the photorefractive transient detection microscope [7], a kind of TDI system, demonstrated visualization of the motion of protozoans while suppressing stationary background.

The phase sensitivity of TDI systems remained initially unexploited, in spite of the fact that phase measurements in biological applications are obviously relevant and background removal considerably helps visualization and measurement. It is worthwhile to mention that photorefractive crystals do have been used traditionally for phase measurement in the area of adaptive interferometers [13–15], in which phase measurements are usually performed in a single spot by signal demodulation, with different applications like remote nondestructive inspection and ultrasonic vibrations measurement. Regarding TDI systems, first investigations on transient phase were reported by Sedlatschek et al. [12] and especially by Krishnamachari and Denz [16], who showed that a TDI system can be used for detecting, as well as measuring, phase changes introduced by moving phase objects. A resolution of $\lambda/20$ at 532 nm was achieved, however the phase measurement range was limited to π rad, due to the inherent ambiguity of

experimental techniques based on direct intensity measurements. A bit later a technique to extend the phase-measurement range was reported [17], based on external phase triggering as often used in the fields of phase-shifting interferometry [18,19] and adaptive interferometry [15].

Since 2003, there has been an advancement of TDI and new applications have been developed, such as particle velocimetry [20], optical tweezers [21], dynamic phase-contrast stereoscopy [22], microfluidic dynamics [23], among others. However, measurements of the transient output phase of the device and its relation with the input phase change have remained unexplored. Previous works rely on conventional intensity measurements, where partial information about input signal phase changes are obtained by previous calibration using an input phase-output intensity transfer function of the particular system.

Here we close that gap by reporting investigation on the TDI output phase and its relation with the input signal phase changes. Output phase is retrieved from off-axis holographic Fourier techniques which, compared to conventional intensity-based TDI, provide important additional features such as directionality of the phase change, higher resolution, and differential-phase measurement for enhanced sensitivity without need of calibration.

2. Theory

We consider two-wave mixing in a photorefractive crystal [1–4,6]. The two coherent beams (pump and signal) propagate co-directionally and intersect at an angle inside the crystal, forming an interference pattern. The resulting intensity grating causes, via the photorefractive effect, a refractive index grating or, in other words, a dynamic volume hologram. Both gratings have the same spatial period but are spatially shifted each other: by default (diffusion-dominated charge transport) the shift is equal to one quarter of a spatial period, but it can be modified with the help of external dc electric fields (drift-driven recording). Denoting the slowly-varying complex amplitudes of the refractive index grating, the signal beam, and the pump beam by $G(z, t)$, $A_1(z, t)$, and $A_2(z, t)$, respectively, being z the bisector between both beams (the crystal extends from $z = 0$ to $z = L$) and t time, the dynamics of grating formation is described by the following relaxation equation [3,6],

$$\frac{\partial}{\partial t} G = \tau^{-1} \left[-G + \frac{1}{2} \Gamma \frac{A_1 A_2^*}{I_0} \right], \quad (1)$$

where τ is a complex time constant, Γ is a complex coupling constant, and $I_0 \equiv I_1 + I_2$ ($I_{i=1,2} = |A_i|^2$) is the sum of intensities. The photorefractive response time strongly depends on the material, and is sensitive to the illumination level [1,16,24]: in ferroelectrics it typically ranges from few milliseconds to hours while in semiconductors it ranges from microseconds for continuous-wave recording [25] to sub-nanosecond level for pulsed recording [26]. As the spatial period of the index grating is self-adjusted to the angle between pump and signal waves, the Bragg condition is automatically satisfied, leading to efficient coupling between both beams. This coupling is however asymmetric because of the spatial shift between index and intensity gratings: the radiation scattered by the index grating interferes constructively with one of the waves and destructively with the other, leading to a net energy flow between them. The spatial evolution of the fields along the crystal is governed by a coupled-mode theory, see e.g. [6], which can be written as

$$\frac{\partial}{\partial z} \mathbf{A} = \mathcal{G} \mathbf{A}, \quad \mathbf{A} = \begin{bmatrix} A_1 \\ A_2 \end{bmatrix}, \quad \mathcal{G} = \begin{bmatrix} -\alpha/2 & -G \\ G^* & -\alpha/2 \end{bmatrix}, \quad (2)$$

being α the background absorption coefficient. Solving Eqs. (2) in steady-state shows [1,6] that the coupling constant $\gamma \equiv \text{Re } \Gamma$, with its sign, explains the strength and direction of energy transfer. In fact, the sign of γ is defined by the direction of the index grating shift relative to the

intensity pattern, which in its turn depends on the orientation of the polar axis of the crystal and of the type of charge carriers, electrons or holes.

A detailed study of the interference between the beams, partially transmitted and partially diffracted by the photorefractive grating, which in particular requires evaluating the effective diffraction efficiency of the volume hologram, allows assessing the performance of TDI [12].

Here we introduce a theoretical approach that exploits the linearity of Eq. (2) with respect to the fields. In this approach there is no need of determining neither the beams profiles nor the crystal parameters, and thus is very convenient for experimental application. In more detail, linearity of Eq. (2) translates into a linear relation between input $\mathbf{A}^{\text{in}}(t) \equiv \mathbf{A}(0, t)$ and outputs $\mathbf{A}^{\text{out}}(t) \equiv \mathbf{A}(L, t)$ via $\mathbf{A}^{\text{out}}(t) = \mathcal{T}(t)\mathbf{A}^{\text{in}}(t)$, where the transfer matrix \mathcal{T} (of elements T_{ij}) represents the effect of the volume hologram. In particular, the output signal field can be calculated as

$$A_1^{\text{out}}(t) = T_{11}A_1^{\text{in}} + T_{12}A_2^{\text{in}}, \quad (3)$$

where the same argument (t) is to be understood in every quantity.

Before detailing our theoretical approach, we note that Eq. (2) ignores the transverse coordinates (x, y) of the beams, precisely where objects and images are codified. This is a usual approximation if diffraction can be neglected along the crystal, which obviously limits the spatial resolution. Hence, in practical terms, any input field distribution $A_1^{\text{in}}(x, y, t)$ –the scene– is transferred to the output $A_1^{\text{out}}(x, y, t)$, while pump is assumed constant across the transverse plane. Obviously, energies and phases get modified. Therefore, one can think of Eq. (3) as being applicable, point to point, from input to output transverse planes.

Let us then assume then that a constant input $\mathbf{A}^{\text{in}} = \bar{\mathbf{A}}^{\text{in}}$ is applied until the index grating reaches a steady-state, characterized by a transfer matrix $\bar{\mathcal{T}}$. [In the following, the overbar will denote steady-state quantities corresponding to $\bar{\mathbf{A}}^{\text{in}}$.] Hence, according to Eq. (3) we have

$$0 = \bar{A}_1^{\text{out}} = \bar{T}_{11}\bar{A}_1^{\text{in}} + \bar{T}_{12}\bar{A}_2^{\text{in}}, \quad (4)$$

where we have expressed that the system is set for steady-state output-signal effective suppression, since we are considering TDI systems. Now we consider alterations of that situation. We assume $\mathcal{T}(t) = \bar{\mathcal{T}}$ in Eq. (3), even following input changes that may occur. This is effectively so whenever changes are fast enough, and last little, as compared to the photorefractive response time, which is key to TDI. So, consider now a TDI situation in which the scene changes to $A_1^{\text{in}} = \bar{A}_1^{\text{in}} + \Delta A_1^{\text{in}}$, and denote by A_1^{TDI} the signal output. Then, from Eqs. (3) and (4),

$$A_1^{\text{TDI}} = \bar{T}_{11}\Delta A_1^{\text{in}}, \quad (5)$$

which shows that, in principle, we need to compute or measure the matrix element \bar{T}_{11} . However, and quite surprisingly, for pure phase variations as we consider even that information is not fully necessary. Instead, a reference signal is measured as follows: while the input signal is in the initial state \bar{A}_1^{in} , we block momentarily the pump ($A_2^{\text{in}} = 0$) and measure the output signal, denoted by A_1^{ref} . According to Eq. (3), $A_1^{\text{ref}} = \bar{T}_{11}\bar{A}_1^{\text{in}}$ and Eq. (5) becomes

$$A_1^{\text{TDI}} = A_1^{\text{ref}}\Delta A_1^{\text{in}}/\bar{A}_1^{\text{in}}. \quad (6)$$

This equation provides a general description of TDI solely based on field measurements. Further it evidences the working principle of TDI: only those parts of a scene undergoing changes are revealed.

In this work we consider cases in which the new input just differs from the old one by a phase shift $\Delta\varphi_1$, i.e. $\Delta A_1^{\text{in}} = \bar{A}_1^{\text{in}}(e^{i\Delta\varphi_1} - 1)$, hence Eq. (6) becomes

$$A_1^{\text{TDI}} = A_1^{\text{ref}}(e^{i\Delta\varphi_1} - 1). \quad (7)$$

From here, the following equation for the output-signal transient phase, defined as $\varphi_T \equiv \arg A_1^{\text{TDI}}$, is obtained:

$$\varphi_T - \varphi_{\text{ref}} = \arg(e^{i\Delta\varphi_1} - 1) = \frac{\Delta\varphi_1}{2} + \frac{\pi}{2} \text{sign}\Delta\varphi_1, \quad (8)$$

with $\varphi_{\text{ref}} \equiv \arg A_1^{\text{ref}}$. This is a main theoretical result, as it relates the transient phase with an input-signal phase change, which we wish to determine. Notably, that relation is piecewise linear (see below). Note that Eq. (8) does not involve measuring any property of the photorefractive crystal; it just relies on output-signal measurements. In other words, while the phases φ_T and φ_{ref} depend in general on the photorefractive crystal and illumination used, their difference, per Eq. (8), is setup insensitive.

For completeness, the expression of the output intensity following from Eq. (7) reads

$$I_1^{\text{TDI}} = 4I_1^{\text{ref}} \sin^2 \frac{\Delta\varphi_1}{2}, \quad (9)$$

which is the basis of the conventional way of inferring the input phase change [12,16,23], and evidences the π ambiguity of the phase inference based on intensity measurements.

Notably, Eq. (8) predicts a π jump in the transient phase $\varphi_T - \varphi_{\text{ref}}$ around $\Delta\varphi_1 = 0$, which is revealed when comparing the transient phases φ_T^\pm corresponding to two arbitrary phase increments, one positive ($\Delta\varphi_1^+ > 0$) and the other negative ($\Delta\varphi_1^- < 0$). The difference $\Delta\varphi_T \equiv \varphi_T^+ - \varphi_T^-$, is then

$$\Delta\varphi_T = \pi + \frac{1}{2}(\Delta\varphi_1^+ - \Delta\varphi_1^-), \quad (10)$$

Hence, even very small phase variations ($\Delta\varphi_1^+ - \Delta\varphi_1^- \rightarrow 0$) around zero are “amplified” to a value of π .

3. Experimental setup

The experimental setup, schematized in Fig. 1, is based on a single-frequency laser emitting at 532 nm with horizontal polarization, and a $5 \times 5 \times 5$ -mm³ strontium-barium niobate (SBN) crystal. The main laser beam is attenuated to 20 mW and then split into three beams: a signal beam, a pump beam, and a reference beam for interferometry. Signal and pump beams intersect at the nonlinear crystal, which has its c^+ -axis oriented in order to get strong energy transfer from signal to pump under steady-state operation, as explained above. Therefore, the output beam contains images when the signal beam changes. For completeness, note that some authors have applied an external phase shift to the pump beam, after writing the initial grating, so as to obtain effective output suppression in TDI systems based on photorefractive materials that are not diffusion-dominated such as lithium niobate [23]. Additionally, the signal beam is reflected onto a piezo mirror (PZT) which allows fine control of phase changes. In more detail, the PZT is connected to a high-voltage amplifier and a function generator that can apply different sort of pulses to the PZT, providing temporal variations with precise phase change on to the crystal. The injection of pulses with a precise phase in to photorefractive wave-mixing systems has been used in the past, including optically controlled location of phase domain by injection of coherent addressing pulses into a photorefractive oscillator [27]. Different attenuators (A) are used for setup optimization.

A target plane is imaged onto the crystal by a telescope (lenses L1 and L2); therefore, the complex field distribution at that plane defines the actual input signal A_1^{in} , i.e. the scene. The

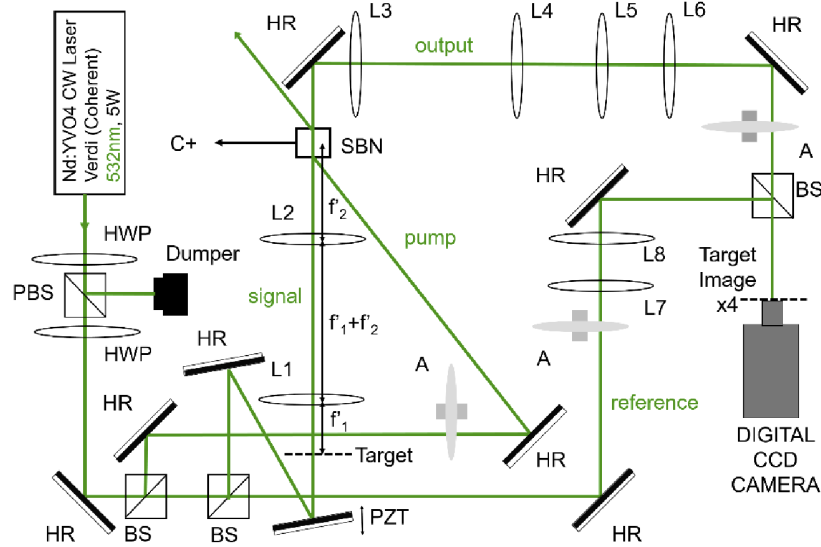


Fig. 1. Experimental setup for interferometric TDI. Signal and pump interact at the SBN photorefractive crystal via TWM. The reference is mixed with the output for interferometry. HWP: half-wave plate. PBS: polarizing beam splitter. HR: high-reflector. BS: beamsplitter. PZT: piezo-mirror. A: attenuator. L1-L8: lenses.

output signal A_1^{out} is finally imaged onto a CCD camera (target image) by a set of lenses (L3-L6). This optical setup provides an input beam magnification $\times 2$, output $\times 4$ and plane phase adjustment.

It is worthwhile to mention that, in this work we do not use any special scene (i.e. a phase object located at the target plane) because our goal here is to present a general new approach to TDI, demonstrate the technique experimentally, and characterize its basic performance. Clearly the results obtained can be extended to spatial variations/motions and phase objects of complex shapes located at the target plane, thanks to the versatility of the experimental setup.

Finally, in order to retrieve the complex amplitude A_1^{out} interference of the output with the reference beam (a tilted plane wave at an angle) is recorded by the CCD camera. Lenses L7-L8 are used to adjust wavefront curvatures and output and reference beam intensities can be attenuated in order to optimize fringe contrast.

4. Experimental procedure

Basically, the experimental procedure consists of applying different signal phase variations and analyzing TDI interferograms. Interferograms recorded by the CCD contain a control zone, where the signal beam does not pass through crystal, and the two-wave mixing (TWM) zone, where signal passes through crystal and interacts with the pump.

The spatial distribution of intensity recorded by the CCD camera is given by the coherent superposition of the output signal field A_1^{out} and the reference tilted wave, of amplitude R and transverse wave number k_R . In terms of the transverse coordinates (x, y) of the CCD plane the interferogram intensity is

$$I(x, y) = |A_1^{\text{out}}(x, y) + Re^{ik_R y}|^2. \quad (11)$$

The analysis and processing of the interferogram is performed in its numerically computed Fourier transform $\tilde{I}(k_x, k_y)$ in terms of the transverse wave numbers (k_x, k_y) . Denoting by $\tilde{F}(k_x, k_y)$

the Fourier transform of A_1^{out} , we have

$$\tilde{I}(k_x, k_y) = \tilde{I}_0(k_x, k_y) + R^* \tilde{F}(k_x, k_y - k_R) + R \tilde{F}^*(-k_x, -k_y - k_R), \quad (12)$$

where $\tilde{I}_0(k_x, k_y)$ is the Fourier transform of the intensity sum $|A_1^{\text{out}}|^2 + |R|^2$. The underlined term of interest is a shifted version of \tilde{F} , whose position on the detection plane is controlled by the reference-wave tilt k_R . Digitally isolating, centering, and performing an inverse Fourier transform, the signal-field complex amplitude A_1^{out} is finally reconstructed. This off-axis digital holographic technique can be used for image analysis such as enhancing intensity image contrast [28], amplitude and phase analysis of patterns [29], and characterization of the nonlinear dynamics of phase domains in photorefractive four-wave mixing oscillators [30].

In this work, we present, for the first time, implementation and use of off-axis digital holography in TDI. Figure 2 shows examples of this interferometric technique in our TDI system. Interferograms correspond to a steady-state situation [Fig. 2(a)] and to a transient state after a fast phase change in the scene [Fig. 2(b)]. The interferogram in Fig. 2(a) shows a dark TWM zone, as a result of the strong attenuation of the output signal in steady-state operation, leading to its effective suppression. As soon as the input signal phase undergoes a change, interference

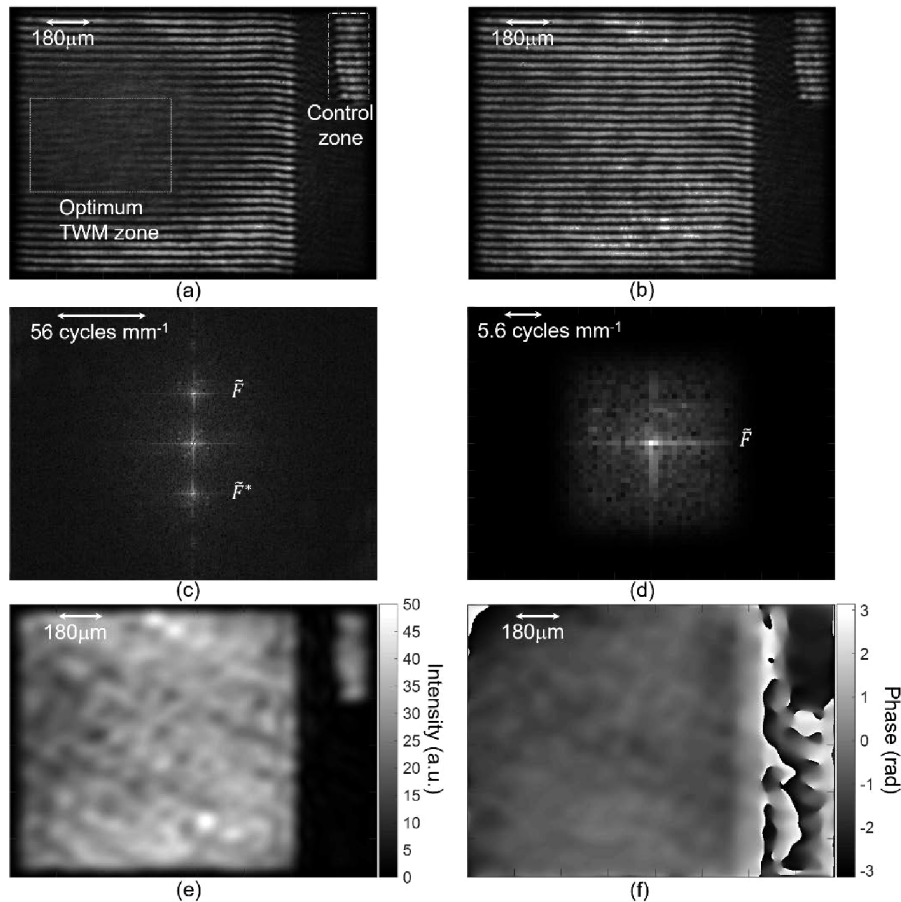


Fig. 2. Interferogram for static 2D phase image (a) Interferogram for dynamic 2D phase image (b) and its Fourier transform (c), upper-order filtered Fourier transform (d), and full 2D retrieval of intensity (e) and phase (f).

fringes emerge in the TWM zone [Fig. 2(b)] as now the signal beam is emerging from the crystal according to Eq. (7). The Fourier transform of the transient interferogram of Fig. 2(b) is shown in Fig. 2(c), which indicates the different terms in Eq. (12). The isolated and spatially filtered Fourier transform is shown in Fig. 2(d) which, via inverse Fourier transform, allows recovering of full 2D amplitude [Fig. 2(e)] and phase [Fig. 2(f)].

5. Results

We analyze the control zone and optimum TWM zone of TDI interferograms by computing mean values and standard deviations (std) for intensities and phases, obtaining $I_1^{\text{TDI}} = 30 \pm 10$ a.u. in Fig. 2(e) and $\varphi_T = -0.92 \pm 0.17$ rad in Fig. 2(f), for a signal phase change $\Delta\varphi_1 = 0.60 \pm 0.10$ rad measured using control zones in Figs. 2(a) and (b).

The signal output phase for static image, $\varphi_{\text{ref}} = -2.81 \pm 0.10$ rad, is obtained by fast blocking of the pump beam. Thus, $\varphi_T - \varphi_{\text{ref}} = 1.89 \pm 0.20$ rad, in agreement with Eq. (8). Note that output intensity is almost zero $I_1^{\text{TDI}} = 3 \pm 3$ a.u. for a static image, see Fig. 2(a), indicating optimum suppression arrangement.

From std analysis, we can conclude that output phase measurements provide more accurate measurements than intensity. Moreover, std for phase retrieval without pump are of the same order (std = 0.11 rad), indicating presence of some noise, probably due to non-homogeneities in the SBN crystal and low signal powers (<1mW); nevertheless, transient-phase measurements seem to be quite robust against such noise levels. Using this complex-field retrieval method, we can investigate the output intensities and phases for different signal input changes.

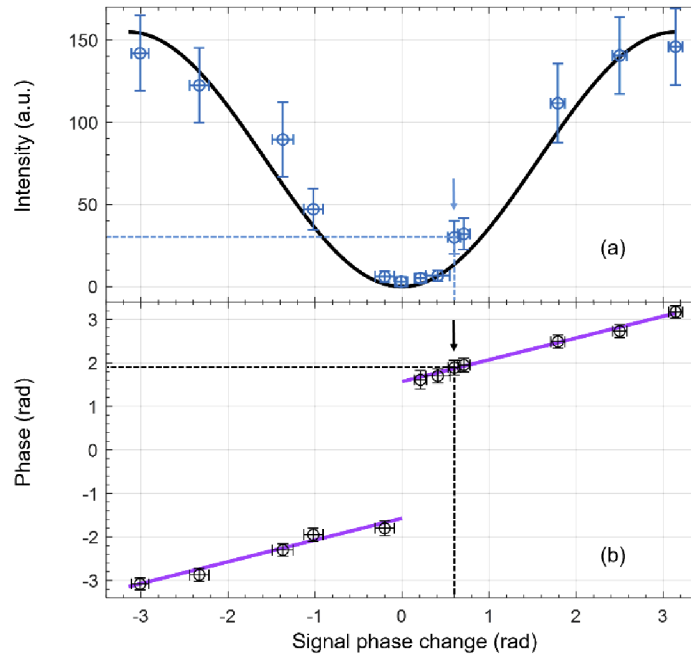


Fig. 3. Transient output intensity (a) and phase (b) corresponding to applied signal-phase change. Plots contain experimental mean values (squares) and the bars show 2-times std errors for measurements in the optimum TWM zone (vertical bars) and control zone (horizontal bars). The solid line in (a) is a fit to Eq. (9), $I_1^{\text{TDI}} = a_1 \sin^2(\Delta\varphi_1/2)$, with $a_1 = 155 \pm 14$ and $R^2 = 0.95$. The solid line in (b) corresponds to Eq. (8): no fitting parameters. Arrows point the case illustrated in Fig. 2.

Figure 3 displays the measured TDI intensity (a) and phase (b) depending on signal phase changes. Such changes are set by applying variable peak voltages to the PZT mirror in the form of signal pulses (50 ms pulse duration, 2s pulse separation) which are short as compared with the response time of the crystal (~ 600 ms). Intensity is fit according to Eq. (9), as reported in previous works [12,16,17,21]. On the contrary, phase measurements do not require a specific fit since experimental points nicely follow the theoretical linear dependence of Eq. (8). Furthermore, phase measurements provide a mean value and std of residuals (difference between the theoretical and experimental signal change for a measured transient phase) of -0.05 ± 0.15 rad achieving a phase measurement precision of $\lambda/30$. Moreover, transient phase detection can measure signal changes from $-\pi$ to π , whereas intensity measurements are ambiguous.

Finally, we demonstrate differential signal-phase measurements applying a very weak alternating signal to the PZT inducing a zero-crossing phase-change (< 0.5 rad). As a result, low intensity transient interferograms appear but with clear fringe changes. Figure 4 presents interferograms in the optimum TWM zone for both positive and negative signal phase changes and complex-field retrievals. Experimental results prove that intensity cannot distinguish between the two

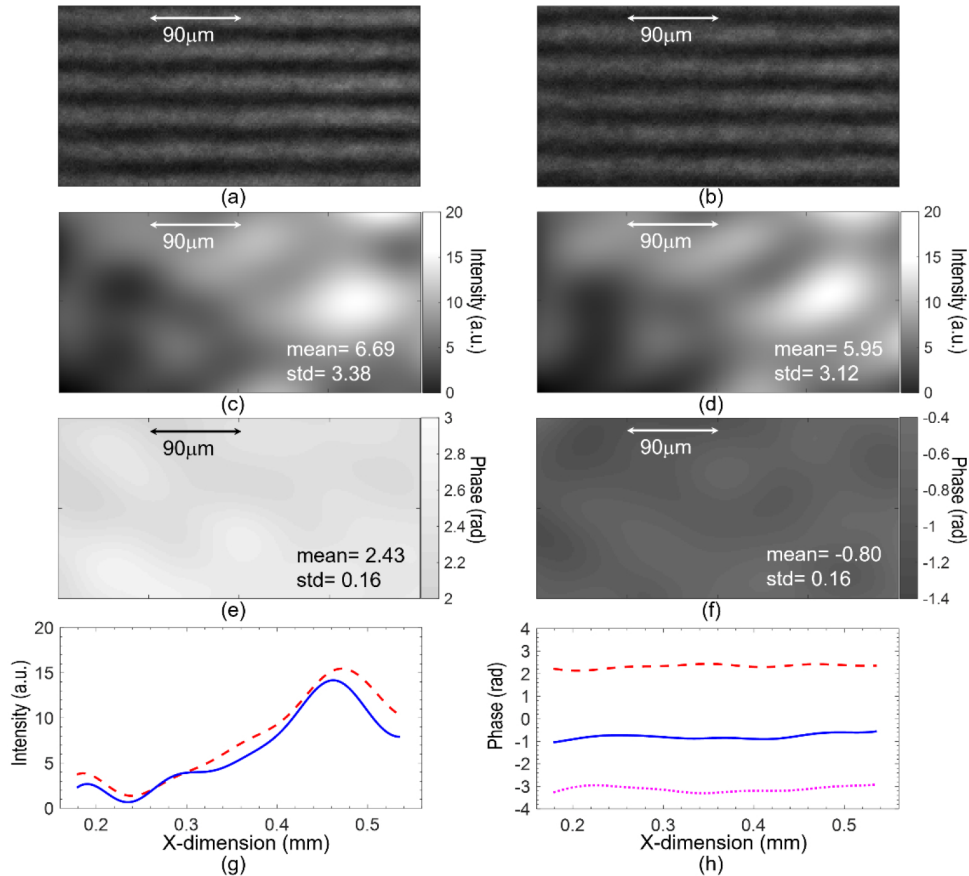


Fig. 4. Complex-field retrieval in differential TDI. Interferograms for positive (a) and negative signal phase changes (b), 2D transient output intensity for positive (c) and negative (d) signal phase changes, 2D transient output phase for positive (e) and negative (f) signal phase changes, 1D intensity (g) and phase (h) profiles for positive (dashed lines) and negative (solid lines) signal phase changes, and differential transient phase (dotted line).

states. However, transient output phases are clearly different with a differential phase of $\Delta\varphi_T = -3.23 \pm 0.23$ rad, between both positions, and demonstrating clear detection with π “amplification” of a weak signal change crossing zero.

6. Conclusion

We have experimentally demonstrated a setup for retrieving the output complex field in TDI. We have evidenced the linear relation existing between input and output phases for the entire range from $-\pi$ to π , in excellent agreement with our theory. The results indicate that phase-change inference from transient phase measurements improves inference from transient intensity measurements, reaching $\lambda/30$ resolution without need of any calibration. Furthermore, we have demonstrated differential-phase detection in TDI, showing the direct measurement of phase changes. Such a technique combines background suppression with extremely-high phase-sign sensitivity, which is especially important for low-power small-phase change signals, and thus demonstrates its potential application as a sensor.

We have reported results based on a photorefractive TDI system with a response time on the order of 1s. Should faster response times be required, it would be worth considering semiconductors pumped by near-infrared lasers, as no fundamental limitation in this respect is expected from our theory.

The linear phase response of TDI represented by Eq. (8) and Fig. 3(b) strongly contrasts with the nonlinear, \sin^2 intensity response to phase changes. In diffusion-dominated photorefractive holograms, such as the ones used here, the illumination and refractive index gratings are relatively shifted by $\pi/2$ so that, for small input phase changes, a negligible (parabolic) change in the output intensity is observed, as reflected in Fig. 3(a). However, the same experiment leads to a strong change in the output phase, which we have exploited here. The intensity response can be improved as in some adaptive interferometers [14,15], where the introduction of a suitable dc-bias in the crystal (drift-driven recording) or of a $\pi/2$ phase shift results in an approximately linear conversion between phase and intensity, in a limited range of input phases. This happens because optimal phase-to-intensity sensitivity is achieved when illumination and refractive index gratings are shifted by π , which can be met by applying a $\pi/2$ square-shaped phase modulation on the signal or pump beams [31,32] in diffusion-dominated photorefractive crystals or by applying an electric bias. We emphasize that the linear phase-to-phase response of TDI given by Eq. (8) is independent of the type of recording, i.e without electric bias (dominated by diffusion) or with it (driven by drift), in clear contrast with adaptive interferometry.

Finally, we believe that this work opens up new possibilities on transient phase detection and its applications.

Funding

Ministerio de Economía, Industria y Competitividad, Gobierno de España, European Regional Development Fund (FEDER)(FIS2017-89748-P, FIS2017-89988-P).

Acknowledgments

We acknowledge fruitful discussions with E. Roldán (Departament d'Òptica i Optometria i Ciències de la Visió, Universitat de València).

Disclosures

The authors declare no conflicts of interest.

References

1. P. Yeh, *Introduction to Photorefractive Nonlinear Optics* (Wiley, 1993).

2. D. L. Staebler and J. J. Amodei, "Coupled-Wave Analysis of Holographic Storage in LiNbO₃," *J. Appl. Phys.* **43**(3), 1042–1049 (1972).
3. N. V. Kukhtarev, V. B. Markov, S. G. Odulov, M. S. Soskin, and V. L. Vinetskii, "Holographic storage in electrooptic crystals.1. Steady-state," *Ferroelectrics* **22**(3-4), 949–960 (1979).
4. N. V. Kukhtarev, V. B. Markov, S. G. Odulov, M. S. Soskin, and V. L. Vinetskii, "Holographic storage in electrooptic crystals.2. Beam coupling-light amplification," *Ferroelectrics* **22**(3-4), 961–964 (1979).
5. M. Cronin-Golomb, A. M. Biernacki, C. Lin, and H. Kong, "Photorefractive time differentiation of coherent optical-images," *Opt. Lett.* **12**(12), 1029–1031 (1987).
6. D. Z. Anderson and J. Feinberg, "Optical novelty filters," *IEEE J. Quantum Electron.* **25**(3), 635–647 (1989).
7. R. S. Cudney, R. M. Pierce, and J. Feinberg, "The transient detection microscope," *Nature* **332**(6163), 424–426 (1988).
8. D. Z. Anderson, D. M. Lininger, and J. Feinberg, "Optical tracking novelty filter," *Opt. Lett.* **12**(2), 123–125 (1987).
9. N. S.-K. Kwong, Y. Tamita, and A. Yariv, "Optical tracking filter using transient energy coupling," *J. Opt. Soc. Am. B* **5**(8), 1788–1791 (1988).
10. P. Mathey, P. Jullien, and D. Rytz, "Efficient contour generation and tracking of a moving object with a rhodium-doped BaTiO₃ crystal working in the near infrared," *Appl. Phys. Lett.* **73**(23), 3327–3329 (1998).
11. M. Esselbach, A. Kiessling, H. Rehn, B. Fleck, and R. Kowarschik, "Transient phase measurement using a self-pumped phase-conjugate mirror as an optical-novelty filter," *J. Opt. Soc. Am. B* **14**(4), 846–851 (1997).
12. M. Sedlatschek, J. Trumppheller, J. Hartmann, M. Müller, C. Denz, and T. Tschudi, "Differentiation and subtraction of amplitude and phase images using a photorefractive novelty filter," *Appl. Phys. B* **68**(5), 1047–1054 (1999).
13. I. Rossomakhin and S. Stepanov, "Linear adaptive interferometers via diffusion recording in cubic photorefractive crystals," *Opt. Commun.* **86**(2), 199–204 (1991).
14. P. Delaye, A. Blouin, D. Drolet, L. A. de Montmorillon, G. Roosen, and J. P. Monchalin, "Detection of ultrasonic motion of a scattering surface by photorefractive InP:Fe under an applied dc field," *J. Opt. Soc. Am. B* **14**(7), 1723–1734 (1997).
15. A. A. Kamshilin, R. V. Romashko, and Y. N. Kulchin, "Adaptive interferometry with photorefractive crystals," *J. Appl. Phys.* **105**(3), 031101 (2009).
16. V. V. Krishnamachari and C. Denz, "Real-time phase measurement with a photorefractive novelty filter microscope," *J. Opt. A: Pure Appl. Opt.* **5**(5), S239–S243 (2003).
17. V. V. Krishnamachari and C. Denz, "A phase-triggering technique to extend the phase-measurement range of a photorefractive novelty filter microscope," *Appl. Phys. B* **79**(4), 497–501 (2004).
18. P. Hariharan, *Optical Holography: Principles, Techniques and Applications* (Cambridge University, 1996).
19. J. Li and H. Fan, "Generalized phase-shifting real-time holography based on photorefractive crystals," *Opt. Las. Eng.* **120**, 79–83 (2019).
20. M. Woerdemann, F. Holtmann, and C. Denz, "Full-field particle velocimetry with a photorefractive optical novelty filter," *Appl. Phys. Lett.* **93**(2), 021108 (2008).
21. M. Woerdemann, F. Holtmann, and C. Denz, "Holographic phase contrast for dynamic-beam optical tweezers," *J. Opt. A: Pure Appl. Opt.* **11**(3), 034010 (2009).
22. F. Holtmann, M. Oevermann, and C. Denz, "Dynamic phase-contrast stereoscopy for microflow velocimetry," *Appl. Phys. B* **95**(3), 633–636 (2009).
23. V. V. Krishnamachari, O. Grothe, H. Deitmar, and C. Denz, "Novelty filtering with a photorefractive lithium-niobate crystal," *Appl. Phys. Lett.* **87**(7), 071105 (2005).
24. G. Montemezzani, C. Medrano, P. Günter, and M. Zgonik, "Charge carrier photoexcitation and two-wave mixing in dichroic materials," *Phys. Rev. Lett.* **79**(18), 3403–3406 (1997).
25. M. B. Klein, "Beam coupling in undoped GaAs at 1.06 μm using the photorefractive effect," *Opt. Lett.* **9**(8), 350–352 (1984).
26. K. Jarasiunas, J. Vaitkus, P. Delaye, and G. Roosen, "Dislocation density-dependent photorefractive effect in (001)-cut GaAs," *Opt. Lett.* **19**(23), 1946–1948 (1994).
27. A. Esteban-Martín, V. B. Taranenko, E. Roldán, and G. J. de Valcárcel, "Control and steering of domain phase walls," *Opt. Express* **13**(10), 3631–3636 (2005).
28. M. Bedrossian, J. Kent Wallace, E. Serabyn, C. Lindensmith, and J. Nadeau, "Enhancing final image contrast in off-axis digital holography using residual fringes," *Opt. Express* **28**(11), 16764–16771 (2020).
29. Y. Larionova, U. Peschel, A. Esteban-Martín, J. García Monreal, and C. O. Weiss, "Ising and Bloch walls of phase domains in two-dimensional parametric wave mixing," *Phys. Rev. A* **69**(3), 033803 (2004).
30. A. Esteban-Martín, M. Martínez-Quesada, V. B. Taranenko, E. Roldán, and G. J. de Valcárcel, "Bistable Phase Locking of a Nonlinear Optical Cavity via Rocking: Transmuting Vortices into Phase Patterns," *Phys. Rev. Lett.* **97**(9), 093903 (2006).
31. K. Shcherbin and M. B. Klein, "Adaptive interferometers with no external field using reflection gratings in CdTe:Ge at 1550 nm," *Opt. Commun.* **282**(13), 2580–2585 (2009).
32. T. J. Hall, M. A. Fiddy, and M. S. Ner, "Detector for an optical-fiber acoustic sensor using dynamic holographic interferometry," *Opt. Lett.* **5**(11), 485–487 (1980).